MOLECULAR AND CELLULAR BIOLOGY, May 1985, p. 1073–1083
0270-7306/85/051073-11$02.00/0
Copyright © 1985, American Society for Microbiology
Vol. 5, No. 5

Overexpressed pp60$^{c\text{-}src}$ Can Induce Focus Formation Without Complete Transformation of NIH 3T3 Cells

PAUL J. JOHNSON, PAUL M. COUSSENS, ANNETTE V. DANKO, AND DAVID SHALLOWAY*

Department of Molecular and Cell Biology, The Pennsylvania State University, University Park, Pennsylvania 16802

Received 7 December 1984/Accepted 14 February 1985

NIH 3T3 cells were transfected with plasmids containing Moloney murine leukemia virus long terminal repeats and either chicken c-*src* or v-*src* genes. In contrast with the effects observed after transfection with plasmids containing c-*src* and avian retrovirus or simian virus 40 promoter-enhancers (H. Hanafusa, H. Iba, T. Takeya, and F. R. Cross, p. 1–8, *in* G. F. Vande Woude, A. J. Levine, W. C. Topp, and J. D. Watson, ed., *Cancer Cells*, vol. 2, 1984; H. Iba, T. Takeya, F. R. Cross, T. Hanafusa, and H. Hanafusa, Proc. Natl. Acad. Sci. U.S.A. 81:4424–4428, 1984; R. C. Parker, R. Swanstrom, H. E. Varmus, and J. M. Bishop, p. 19–26, *in* G. F. Vande Woude et al., ed., *Cancer Cells*, vol. 2, 1984; R. C. Parker, H. E. Varmus, and J. M. Bishop, Cell 37:131–139, 1984; D. Shalloway, P. M. Coussens, and P. Yaciuk, p. 9–17, *in* G. F. Vande Woude et al., ed., *Cancer Cells*, vol. 2, 1984; D. Shalloway, P. M. Coussens, and P. Yaciuk, Proc. Natl. Acad. Sci. U.S.A. 81:7071–7075; and K. C. Wilhelmsen, W. G. Tarpley, and H. M. Temin, p. 303–308, *in* G. F. Vande Woude et al., ed., *Cancer Cells*, vol. 2, 1984), we found that both types of Moloney murine leukemia virus long terminal repeat-*src* expression plasmids induced focus formation, although c-*src* induced only 1% as many foci as v-*src*. The focus-selected c-*src* overexpressed cells had altered morphology and limited growth in soft agarose but were not tumorigenic in vivo. Cleveland digests, comparative in vitro kinase assays, secondary transfections, and immunoprecipitations indicated that focus formation was caused by rare transfection events that resulted in very high-level pp60$^{c\text{-}src}$ expression rather than by mutations of the transfected c-*src* genes. These results suggest that pp60$^{v\text{-}src}$ induced transformation is not a completely spurious activity which is unrelated to the function of pp60$^{c\text{-}src}$ but that it represents a perturbation of already existent molecular control processes involving pp60$^{c\text{-}src}$.

The discovery that the transforming activities of the rapidly transforming RNA tumor viruses are due to oncogenes which have been generated by recombination between cellular and viral nucleotide sequences focused attention on the roles of the homologous cellular proto-oncogene sequences. Most proto-oncogenes are highly conserved in evolution and are expressed at low levels to produce normal cellular proteins. In many cases, the levels of proto-oncogene expression are far below the levels of oncogene product expression associated with viral infection. Therefore, early studies investigated whether oncogene-induced transformation was due to overexpression of functionally normal proteins (or domains) or whether functional modifications of the normal proteins were required.

This question was answered for the cases of the c-*mos*, c-Ha-*ras*, c-*fos*, and c-*src* proto-oncogenes by transfecting tissue culture cells with recombinant expression plasmids that induced relatively high-level proto-oncogene expression (3, 9, 12, 14, 20, 22–24, 28, 29, 35). The plasmids were constructed by replacing proto-oncogene flanking sequences with viral transcriptional enhancers, promoters and polyadenylation signals. Although overexpression of the c-Ha-*ras*, c-*mos*, and c-*fos* protein products induced focus formation in monolayer culture (and, in at least one case, induced in vivo tumorigenicity) overexpression of c-*src* did not, demonstrating that the v-*src* and c-*src* protein products are functionally distinct. However, chicken c-*src* expression in NIH 3T3 mouse cells to levels comparable with virally induced v-*src* expression was shown to cause some morphological alteration and limited growth in soft agarose (28).

Both c-*src* and v-*src* are translated into 60-kilodalton (kd) proteins pp60$^{c\text{-}src}$ and pp60$^{v\text{-}src}$. Both proteins are phosphorylated at serine and tyrosine residues and, along with many activated growth factor receptors (see reference 13 for a review), are plasma membrane-bound tyrosine-specific protein kinases (see references 1 and 2 for a review). Transformation by pp60$^{v\text{-}src}$ induces an eightfold increase in the total amount of cellular phosphotyrosine (26). In contrast, the protein tyrosine kinase activity of pp60$^{c\text{-}src}$ is restricted in intact cells, and overexpression of pp60$^{c\text{-}src}$ to levels comparable to those of pp60$^{v\text{-}src}$ in transformed cells does not induce a commensurate increase in total cell phosphotyrosine (6a, 13a).

pp60$^{v\text{-}src}$ transforms cells from a wide range of animals, including chickens, rodents, and humans (see reference 11 for a review). This may be related to the fact that at least the carboxyl domains of the c-*src* proteins from these species are highly conserved: only 12 isolated substitutions in the 419 carboxyl amino acids of the two proteins distinguish the inferred protein sequences of chicken and the sequenced variant of human pp60$^{c\text{-}src}$ (33; D. Fujita and H.-J. Kung, personal communication).

In contrast to other known oncogenes, which are chimeras of viral and cellular sequences, v-*src* is composed almost exclusively of chicken cellular sequences, and the chicken pp60$^{c\text{-}src}$ and pp60$^{v\text{-}src}$ proteins differ only in a small exchange of sequences at the carboxyl termini (19 amino acids in pp60$^{c\text{-}src}$ are replaced by 12 amino acids in pp60$^{v\text{-}src}$) and a number of scattered amino acid substitutions (33). The scattered substitutions are not required for transformation, and replacement of the carboxyl end of pp60$^{c\text{-}src}$ with the corresponding sequence from pp60$^{v\text{-}src}$ creates a transforming protein. On the other hand, the specific sequence at the carboxyl end of pp60$^{v\text{-}src}$ is also not required for transforma-

* Corresponding author.

tion, since other mutated *src* proteins having different carboxyl termini also have transforming activity, and some but not all chimeric 5′v-*src*–3′c-*src* constructs induce transformation with high efficiency (12, 14, 28, 29).

pp60$^{c\text{-}src}$ may play an important role in transformation by polyomaviruses as well as retroviruses. Polyoma middle T antigen binds to pp60$^{c\text{-}src}$ in vivo (7) and polyoma virus infection induces enhanced tyrosine kinase activity and the appearance of a new phosphotyrosine residue in pp60$^{c\text{-}src}$ (4). It seems likely that the function of middle T antigen in polyoma virus-induced transformation is mediated by the associated activation and possible modification of pp60$^{c\text{-}src}$ tyrosine kinase activity.

Since pp60$^{c\text{-}src}$ shares functional properties associated with growth factor receptors and can be involved in transformation either by mutation or by association with an exogenous protein, the examination of its function in cells will be valuable in the study of the molecular mechanisms of transformation. In this paper we show that the effects of pp60$^{c\text{-}src}$ at very high levels of overexpression (about 7 to 10 times the levels of pp60$^{v\text{-}src}$ in transformed NIH 3T3 cells) differ from those observed in previous studies at more moderate expression levels and that pp60$^{c\text{-}src}$ can induce focus formation and some other aspects of transformation without inducing a completely transformed phenotype.

MATERIALS AND METHODS

Plasmids. Plasmids pMc*src* and pMv*src* were constructed by standard recombinant DNA techniques (19). pMc*src* was constructed by gel purifying the 8.1-kilobase (kb) *Bam*HI c-*src* fragment running from c-*src* coordinates −2.1 to 6.0 kb (30) and ligating it into plasmid pEVX (15) DNA which had been linearized at a unique *Bgl*II site lying between the two Moloney murine leukemia virus (MoMLV) long terminal repeats (LTRs). The upstream *Bam*HI site is about 270 base pairs (bp) upstream from the beginning of c-*src* exon no. 2 (unpublished data), whereas the downstream site lies about 1.2 kb beyond the c-*src* termination codon (33). Ligation was performed by using a 10:1 insert-vector DNA fragment molar ratio. The construction was verified by restriction endonuclease mapping.

pMv*src* was constructed in the same manner, except that the 3.1-kb *Bam*HI-*Bgl*II Schmidt Ruppin A v-*src* fragment from plasmid pN4 (14) was inserted into the pEVX *Bgl*II site. This fragment contains 276 bp of pBR322 DNA from the pBR322 *Bam*HI to *Sal*I sites followed by 2.8 kb of Rous sarcoma virus (RSV) DNA from the *Sal*I site that is about 750 bp upstream of the *env* termination codon down to the *Nru*I site that is about 90 bp downstream of the v-*src* termination codon (8, 25, 32). (The *Nru*I site was converted to a *Bgl*II site in the construction of pN4 [14].)

Tissue culture and tissue culture assays. NIH 3T3 cells were grown and transfected in normal or selective media with 10% calf serum as described by Shalloway et al. (28), except that Dulbecco modified Eagle medium (GIBCO Laboratories, Grand Island, N.Y.) was substituted for Temin modified Eagle medium. pEVX, pMv*src*, and pMc*src* were linearized at unique *Sal*I or *Nru*I sites, p*src*11 was linearized at a unique *Hin*dIII site, and pSV302 was linearized at a unique *Pvu*I site; these sites all lie in the pBR322-derived regions of the plasmids. Foci were counted 12 to 14 days after exposure to DNA.

Cells were coselected for Eco-*gpt* expression by trypsinizing the cells 2 days after cotransfection with the Eco-*gpt* expression plasmid pSV302 and transferring the cells from each 60-mm plate to a 100-mm plate containing selective medium (a 1:2.8 dilution). Transfected cells were cloned either from foci or from Eco-*gpt*-selected colonies by using cloning cylinders at 13 to 18 days after transfection. Eco-*gpt* selected cells were frozen down after approximately seven passages, and in all further experiments we used freshly thawed cells which had undergone less than 3 post-thaw passages. Coselected cells were grown and frozen in selective medium and "weaned" into normal media, as described by Shalloway et al. (28), at least 3 days before biological or biochemical assays so that all cell lines were compared in normal media.

Colony formation in soft agarose at 5 and 10% serum concentrations was assayed as described by Shalloway et al. (28).

Biologically cloned cell lines were assayed for focus-forming activity by cell mixing experiments in which either 50, 500, or 5,000 test cells were mixed with 5×10^5 normal NIH 3T3 cells, plated in 60-mm tissue culture dishes in media containing either 5 or 10% serum, and assayed for the appearance of cell foci after 7 to 10 days. We used plates containing 10 to 100 foci per plate to determine focus-forming efficiency by dividing the number of foci 10 to 12 days after mixing by the number of test cells added to the plate. Four independent experiments were carried out for cell lines NIH (pMv*src*/focus-selected)A [NIH(pMv*src*/focus)A], NIH (pMv*src*/coselected)A [NIH(pMv*src*/cos)A], NIH (pMc*src*/focus)B, and NIH(pMc*src*/cos)B. Two independent experiments were carried out for all other cell lines except NIH(pMv*src*/focus)B and NIH(pMv*src*/focus)C, which were only used in one experiment.

[^{35}S]methionine-labeled immunoprecipitations. Cells were plated at 5×10^5 cells per 60-mm plate at 20 h before metabolic labeling in 1 ml of minimal essential medium without methionine (GIBCO) and containing 5% calf serum and 100 μCi of [^{35}S]methionine per ml (>1,000 Ci/mmol; New England Nuclear Corp., Boston, Mass.). (Similar results were obtained [data not shown] in media supplemented with 5% methionine-containing medium.) Cells were lysed in 0.3 ml of RIPA buffer (1% Triton X-100, 1% sodium deoxycholate, 0.1% sodium dodecyl sulfate [SDS], 150 mM NaCl, 20 mM Tris-hydrochloride [pH 7.2]) containing 100 KIU of aprotinin per ml (Sigma Chemical Co., St. Louis, Mo.) and 1 mM phenylmethylsulfonyl fluoride. Total cell protein was determined by using the Bio-Rad Protein Assay. The lysates were clarified at 25,000 × *g* for 30 min, and 200 μg of total cell protein (40 to 50% of total lysate) adjusted to constant volume was used per reaction. Lysates were preabsorbed with 30 μl of a 10% suspension of fixed protein A containing *Staphylococcus aureus* cells for 20 min at 0°C and immunoprecipitated (45 min, 0°C) with 3 μl of rabbit antibody prepared against bacterially produced pp60$^{v\text{-}src}$ (generously donated by J. Brugge). Antibody titers showed this amount of antiserum to provide antibody in excess. The immune complexes were collected on 30 μl of *S. aureus* suspension for 20 min at 0°C, washed 3 times with RIPA, twice with high-salt buffer (1 M NaCl, 0.5% Triton X-100, 10 mM Tris-hydrochloride [pH 7.2]), and twice with KSCN wash (0.75 M KSCN, 0.5% Triton X-100, 10 mM Tris-hydrochloride [pH 7.2]). The final pellets were resuspended in electrophoresis buffer and analyzed by electrophoresis on SDS-10% polyacrylamide gels by using the buffer system described by Laemmli (16). Labeled bands were detected by fluorography of dried gels by using En^{3}Hance (New England Nuclear) and 2- to 10-day exposures.

Cleveland digests. NIH 3T3 cells were labeled and im-

munoprecipitated as described above except that labeling was in Dulbecco modified Eagle medium without phosphate (GIBCO Laboratories) containing 5% calf serum and 0.5 mCi of $H_3{}^{32}PO_4$ per ml (New England Nuclear) for 6 h. Chicken embryo fibroblasts were labeled in Dulbecco modified Eagle medium without phosphate plus 30% tryptose phosphate broth (Difco Laboratories, Detroit, Mich.), 5% calf serum, 2% fetal calf serum, and 0.5 mCi of $H_3{}^{32}PO_4$ for 6 h (inadvertant inclusion of tryptose phosphate broth in this medium resulted in low specific activity of the chicken cell proteins; see Fig. 5.) Cell lysates were prepared and immunoprecipitated as described above. The pp60^{src} bands were identified by autoradiography, excised from dried gels, and subjected to partial proteolytic digestion with 150 ng of *S. aureus* V-8 protease, as described by Cleveland et al. (6). Electrophoresis was carried out on 12.5% SDS-polyacrylamide gels with a 3% stacking gel by using the buffer system described by Laemmli (16). Autoradiography of dried gels was performed at −70°C with a Dupont Cronex enhancing screen and a 1-month exposure.

In vitro kinase assay. The exogenous substrate kinase assays were performed as described by P. M. Coussens et al. (submitted for publication) by using 0.5 μl of monoclonal antibody MAb327 (a generous gift of J. Brugge) (18), 1 μM [γ-^{32}P]ATP, and 0.1 μg of rabbit muscle enolase (type IV; Sigma) per μl. Products of the immune complex kinase reaction were eluted from the *S. aureus* solid-phase support by adding an equal volume of 2× electrophoresis buffer and loading both the material originally in the immune complex and that in the kinase reaction solution onto a 10% SDS-polyacrylamide gel by the method of Laemmli (16). Phosphorylated bands were detected by 4-h autoradiography of the dried gel.

RESULTS

Reasoning that a murine retroviral LTR would be more effective in mouse cells than either the avian (RSV) or primate (simian virus 40) promoters which had previously been used in expression plasmid constructions, we cloned both the chicken c-*src* and Schmidt Ruppin A v-*src* genes into the MoMLV LTR expression plasmid pEVX (15), creating plasmids pMc*src* and pMv*src* (Fig. 1). The *src* genes were inserted downstream from the MoMLV splice donor site so that mRNAs initiated at the LTR cap site would be spliced to connect the MoMLV splice donor to the splice acceptor of c-*src* exon no. 2 (containing the c-*src* AUG [33]) or the splice acceptor found 75 bp upstream from the v-*src* AUG (8, 25, 31, 32). Unlike the situation in RSV, there is no AUG in the MoMLV mRNA region preceding the splice donor site, so we expected translational initiation to occur at the appropriate c-*src* and v-*src* AUGs. The coding sequences in both constructions are followed by a second MoMLV LTR to provide polyadenylation signals. The plasmid constructions are described above.

Primary transfections. The plasmids were transfected into NIH 3T3 cells and assayed for focus-forming activity (Table 1). The focus-forming activities of pMc*src* and pMv*src* were compared with that of the RSV LTR Schmidt-Ruppin D v-*src* expression plasmid p*src*11, which has already been shown to induce transformation in NIH 3T3 cells (28, 29); A. D. Zelenetz and G. M. Cooper, unpublished results). pEVX, the plasmid vector containing MoMLV LTRs with no *src* coding sequence, was used for a negative control.

Multiple transfection experiments with duplicate plates were performed. After initial pilot experiments, quantitative focus-forming activities were determined by using 0.001

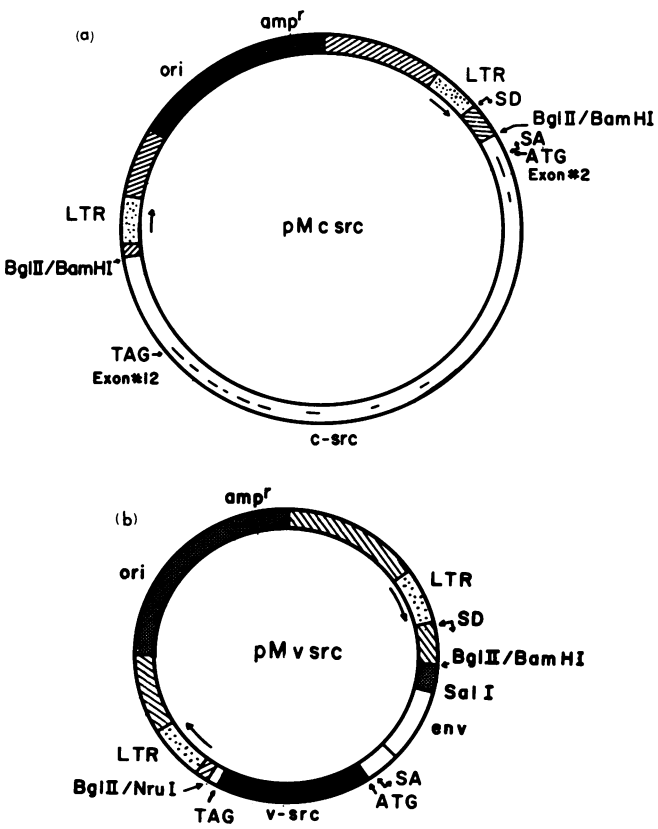

FIG. 1. MoMLV LTR *src* expression plasmids pMc*src* and pMc*src*. The plasmids contain DNAs from the MoMLV expression plasmid pEVX and the chicken c-*src* gene or Schmidt-Ruppin A v-*src* gene. The *src* fragments were inserted at a *Bgl*II site lying between the upstream MoMLV LTR and splice donor (SD) and the downstream MoMLV LTR. (a) pMc*src* contains the c-*src* 8.1-kbp *Bam*HI fragment which runs from 272 bp upstream of the c-*src* exon no. 2 splice acceptor (SA) to 1.2 kbp downstream from the c-*src* termination codon. Lines in the center of the open region show the positions of the c-*src* exons. Length, 14.5 kbp. (b) pMv*src* contains the Schmidt-Ruppin A v-*src* fragment which runs from the *Sal*I site in *env* to the *Nru*I site 90 bp downstream of the v-*src* termination codon. The fragment was derived from plasmid pN4 (14) and also contains 276 bp of pBR322 DNA. Length, 9.5 kbp. Symbols: fine dots, pBR322-derived DNA; coarse dots, MoMLV LTR; crosshatch, mouse genomic, MoMLV, or cloning site insert DNA; open (a), c-*src* DNA; open (b), RSV DNA; solid, v-*src* DNA.

(pMv*src*), 0.01 (p*src*11), and 0.1 μg (pMc*src* and pEVX) of linearized plasmid DNA plus 20 μg of calf thymus carrier DNA per 60-mm tissue culture plate. Different amounts of DNA per plate were used to maintain the number of foci per plate in the linear response range of 0 to 100. pMv*src*, which contains MoMLV LTRs and Schmidt-Ruppin A v-*src*, had about 15 times the focus-forming activity of p*src*11, which contains RSV LTRs and Schmidt-Ruppin D v-*src*. In contrast with previous results in rodent cells with simian virus 40 enhancer/early promoter–c-*src* chimeric plasmids (23, 24, 28, 29), we found that c-*src* overexpression could induce focus formation at low frequency: pMc*src*-induced focus formation with about 1% the molar activity of pMv*src*. pEVX induced one rare focus.

Since the pMv*src* and pMc*src* plasmids are functionally similar in construction, transfection of both plasmids probably caused the same number of independent plasmid DNA integration and expression events. Although some differ-

TABLE 1. Transfection data[a]

Primary Transfection		Secondary Transfection	
DNA	No. of foci/pmol	DNA	No. of foci/μg
Carrier (calf thymus DNA)		NIH 3T3	<0.01
p*src*11	2×10^4		
pEVX	<20		
pMv*src*	3×10^5	NIH(pMv*src*/focus)A	2.2
		NIH(pMv*src*/focus)B	1.3
		NIH(pMv*src*/cos)A	1.5
pMc*src*	3×10^3	NIH(pMc*src*/focus)A	0.03
		NIH(pMc*src*/focus)B	0.04
		NIH(pMc*src*/focus)C	0.05
		NIH(pMc*src*/cos)A	0.02
		NIH(pMc*src*/cos)B	0.02
		NIH(pMc*src*/cos)C	0.03

[a] Focus-forming efficiencies of linearized plasmid DNAs (plus 20 μg of carrier DNA per plate) were determined from multiple experiments with duplicate plates. Plasmid DNA (0.001 to 0.1 μg) was transfected per 60-mm plate such that 0 to 100 foci per plate were generated. The number of foci per picomole were determined from the lengths of the plasmids (in kilobase pairs): p*src*11, 7.8; pEVX, 6.4; pMv*src*, 9.5; pMc*src*, 14.5. NIH(pMc*src*/focus)A, NIH(pMc*src*/focus)B, and NIH(pMc*src*/focus)C are cell lines isolated from pMc*src*-induced foci. NIH(pMc*src*/cos)A, NIH(pMc*src*/cos)B, and NIH(pMc*src*/cos)C are coselected cells lines isolated by picking xanthine-guanine phosphoribosyl transferase-positive colonies after cotransfection with plasmids pMc*src* and pSV302 (a plasmid containing Eco-*gpt*). Similar nomenclature is used for the pMv*src* transfected cell lines.

ences could be associated with the c-*src* introns, previous experiments with the c-*src*–v-*src* chimeric plasmid pRS3 which contains 10 out of the 11 c-*src* introns showed that introns do not significantly reduce focus-forming activity [28]). Thus, it is likely that the pMc*src*-transfected NIH 3T3 cells contained a large population of transfected c-*src* overexpressor cells which did not form foci.

Additional experiments were conducted to determine what distinguished the focus-forming from non-focus-forming pMc*src*-transfected cells. We were particularly interested in investigating two hypotheses. One was that authentic chicken $pp60^{c\text{-}src}$ can induce focus formation in mouse cells when expressed at levels above a relatively sharp high threshold. In this case our experiments would be interpreted as showing that only 1% of the stable pMc*src* transfection events induce expression levels that are above the c-*src* focus-forming threshold compared with the number of pMv*src* events which induce expression levels that are above a lower v-*src* focus-forming threshold. The variation in expression levels might be due to clonal variations among the transfected NIH 3T3 cells, differences in the chromosomal sites of plasmid integration, differences in integrated plasmid copy number, etc. An alternative hypothesis was that the relatively rare c-*src*-induced focus formation was the result of mutations in the integrated c-*src* coding sequences and did not represent the activity of authentic $pp60^{c\text{-}src}$. The latter possibility was suggested by the work of Hanafusa et al. (12) and Iba et al. (14), who showed that c-*src* mutation during the course of retrovirally mediated c-*src* overexpression can induce transformation of chicken cells. In addition, the experiments of Calos et al. (5), Wake et al. (34), and Lebkowski et al. (17) have shown that transfected plasmids may undergo high mutation rates. Although our experiments with nonreplicating plasmids did not involve any error-prone reverse transcription or episomal replication events, the possibility that focus formation was due to c-*src* mutations generated in the transfection event could not be ruled out a priori.

Four types of experiments were carried out to determine whether rare high-level overexpression or mutation was responsible for c-*src* focus formation: (i) comparison of expression levels between coselected and focus-selected c-*src* overexpressor cells, (ii) comparison of Cleveland digests of $pp60^{c\text{-}src}$ from coselected and focus-selected cells with endogenous chicken $pp60^{c\text{-}src}$, (iii) comparison of the in vitro kinase activities of $pp60^{c\text{-}src}$ from coselected and focus-selected cells, and (iv) focus-forming assays in secondary transfections with cellular DNAs from coselected and focus-selected c-*src* overexpressor cells.

Comparison of expression levels between coselected and focus-selected c-*src* overexpressor cells. To sample the population of non-focus-forming c-*src* overexpressor cells pMc*src* DNA was cotransfected with plasmid pSV302, a modified form of pSV2gpt (21), which induces expression of the Eco-*gpt* gene and permits biological selection for xanthine-phosphoribosyl-transferase activity. A 0.1-μg amount of linearized pMc*src* DNA, an equimolar amount of linearized pSV302 DNA, and 20 μg of carrier DNA were used per plate of cells. Colonies of transfected cells expressing Eco-*gpt* activity were cloned in selective media and maintained in subconfluent plates throughout the procedure to minimize selective pressure for high-density cell growth. Three independent cell lines NIH(pMc*src*/cos)A, NIH(pMc*src*/cos)B, and NIH(pMc*src*/cos)C were isolated. All three lines were found to be overexpressing $pp60^{c\text{-}src}$ (see below) and, as previously observed with cells transfected with the simian virus 40 promoter/enhancer–c-*src* chimeric plasmid pCS12.13 (28, 29), had morphologies that were intermediate between normal and v-*src* transformed cells (Fig. 2).

Lysates were prepared from all six NIH(pMc*src*/focus) and NIH(pMc*src*/cos) cell lines after 6 to 8 h of in vivo labeling with [^{35}S]methionine and were immunoprecipitated by using cross-reactive anti-v-*src* serum. Lysate volumes were adjusted to provide equal amounts of total cell protein in each immunoprecipitation reaction. (Specific activities, were equal to within 25%.) The serum (kindly donated by J. Brugge) was prepared by using bacterially produced Pr-A v-*src* (10) and is highly reactive with $pp60^{c\text{-}src}$. Immunoprecipitations from normal NIH 3T3 cells and NIH(p*src*11), a cell line isolated from a p*src*11-induced focus, were used for negative and positive controls. The results are shown in Fig. 3.

It is striking that the focus-selected c-*src* overexpressor cells showed much higher $pp60^{src}$ levels than either the coselected c-*src* overexpressor cells or the p*src*11 v-*src*-transformed cells. (Averaging of the results of densitometer tracings of two experiments of this type showed that the c-*src* focus-selected/c-*src* coselected/v-*src* focus-selected protein ratios were about 4.8:1.2:1). The levels within the classes of cell lines were similar, showing that the differences between the coselected and focus-selected cells were systematic and not random effects.

Parallel control experiments were performed with plasmid pMv*src* (data not shown). In contrast with the results with pMc*src*, the levels of $pp60^{src}$ in the NIH(pMv*src*/focus) and the NIH(pMv*src*/cos) cell lines were all approximately equal, indicating that the differences seen between the c-*src* coselected and focus-selected lines were not artifacts of the selection process.

Since the in vivo half-lives of Schmidt-Ruppin $pp60^{v\text{-}src}$ and $pp60^{c\text{-}src}$ are about 7 to 11 and 20 to 24 h, respectively (13a, 24, 27), these short-term labeling experiments provide a rough indication of the comparative *src* synthesis rates in these cells. (The observed c-*src*/v-*src* ratios should be cor-

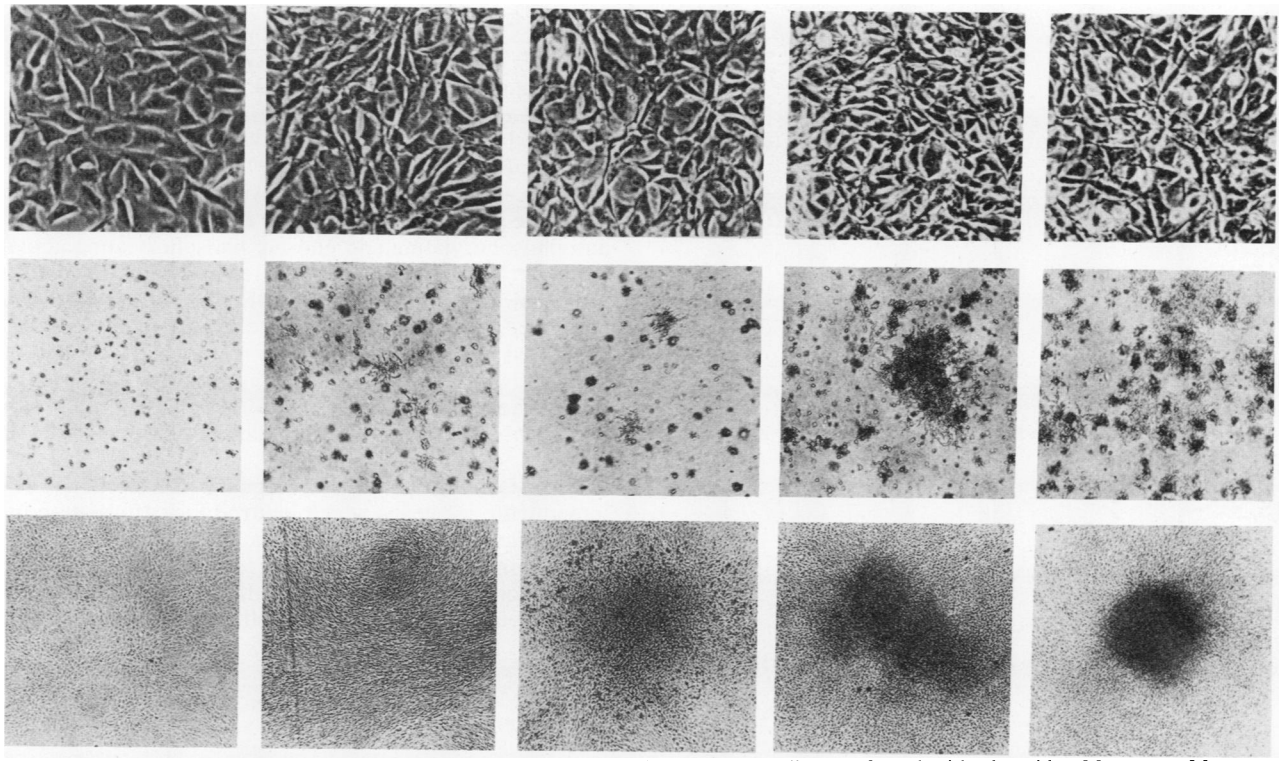

FIG. 2. Biological comparison of c-*src* and v-*src* overexpressor cells. NIH 3T3 cells transfected with plasmids pMc*src* or pMv*src* were biologically cloned after selection by focus formation or by coselection after cotransfection with an Eco-*gpt*-containing plasmid, pSV302. Pictures from only one representative line of each type are shown, as only small variations were observed between different lines within each category. From left to right, the cell lines used were NIH 3T3, NIH(pMc*src*/cos)B, NIH(pMc*src*/focus)C, NIH(pMv*src*/cos)A, and NIH(pMv*src*/focus)A. Top row, cell morphology in monolayer culture; middle row, growth in semisolid medium (10 days after suspension in medium containing 0.25% soft agarose); and bottom row, focus formation in cell mixing experiments [a nonfocal region of morphologically distinctive cells of the type which occurs with low frequency after cell mixing the NIH(pMc*src*/cos) cells is shown in that panel].

rected by a factor of 0.8 to compensate for the use of a labeling time which was relatively long compared with the pp60$^{v\text{-}src}$ half-life.) The fact that only cells selected on the basis of c-*src*-induced focus formation had extremely high protein levels suggested that high-level pp60$^{c\text{-}src}$ synthesis rather than c-*src* mutation was responsible for pMc*src*-induced focus formation and that selection for c-*src* focus formation in these experiments constituted de facto selection for high-level pp60$^{c\text{-}src}$ synthesis.

Cellular and viral pp60^{src} were also immunoprecipitated from both coselected and focus-selected cell lines after 48 h of metabolic labeling with [^{35}S]methionine to compare the equilibrium pp60^{src} levels. The results for cell lines of each type are shown in Fig. 4. Multiple experiments showed that about twice as much pp60$^{c\text{-}src}$ was immunoprecipitated from the c-*src* focus-selected lines relative to the c-*src* coselected lines, whereas equal amounts of protein were immunoprecipitated from the v-*src* focus-selected and coselected lines. It is interesting that the NIH(pMc*src*/cos)A pp60$^{c\text{-}src}$ level was about 5 times that of the NIH(p*src*11) pp60$^{v\text{-}src}$ level, in contrast with the results from the short-term labeling experiments in which the ratio was 1.5:1, reflecting differences in in vivo stability of the proteins. The pp60$^{c\text{-}src}$ level in the focus-selected cells was also elevated [relative to NIH(p*src*11)] and was about 7 to 10 times the NIH(p*src*11) level of pp60$^{v\text{-}src}$. Similarly, the level of endogenous mouse pp60$^{c\text{-}src}$ was elevated and generated bands that can be seen to form doublets with the faster-mobility pp60$^{v\text{-}src}$ bands from plasmids p*src*11 and pMv*src*, in lanes 2, 6, and 7 of Fig. 4. These endogenous mouse pp60$^{c\text{-}src}$ bands provide internal supplementary references for quantitative comparisons of expression levels.

These quantitations are subject to the caveat that cross-reactive antisera generated against pp60$^{v\text{-}src}$ have been used to quantitate three distinct proteins, and differences in reactivity could have suppressed the mouse pp60$^{c\text{-}src}$ signal relative to that of chicken pp60$^{c\text{-}src}$ or pp60$^{v\text{-}src}$. However, we believe that these values are accurate since (i) under identical conditions of antibody excess, large amounts of mouse pp60$^{c\text{-}src}$ (the potentially weakest antigen) were immunoprecipitated relative to pp60$^{v\text{-}src}$ (the potentially strongest antigen), and (ii) similar quantitative results were obtained in [^{35}S]methionine-labeled immunoprecipitations with cross-reactive monoclonal *src* antibody MAb 327 (18; data not shown).

Comparison of Cleveland digests of pp60$^{c\text{-}src}$ from coselected and focus-selected overexpressor cells. ^{35}S immunoprecipitations showed that the pp60$^{c\text{-}src}$ proteins immunoprecipitated from all six c-*src* overexpressor lines comigrated with an apparent molecular weight of 60,000 and slightly slower mobility than Schmidt-Ruppin D pp60$^{v\text{-}src}$, consistent with overexpression of authentic pp60$^{c\text{-}src}$ in all the c-*src* lines. To provide more accurate comparison, these lines were metabolically labeled with ^{32}P and the immunoprecipitated c-*src* proteins were analyzed by Cleveland digestion with *S. aureus* V-8 protease. The patterns from all six lines were

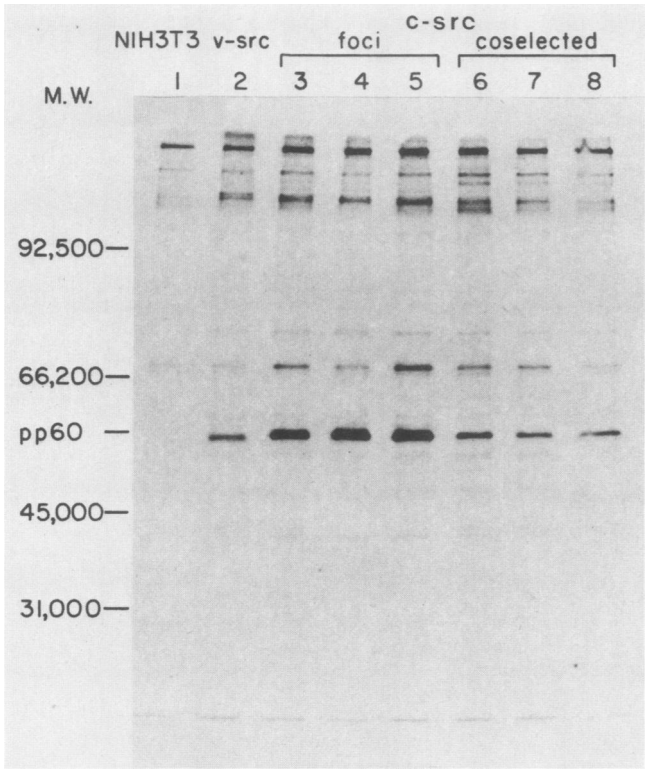

FIG. 3. Comparative pp60$^{c\text{-}src}$ immunoprecipitations from focus-selected and coselected c-*src* overexpressor cells; short-term label. Cells from biological clones (1) NIH 3T3; (2) NIH(p*src*11); (3) through (5) NIH(pMc*src*/focus-selected)A, NIH(pMc*src*/focus)B, and NIH(pMc*src*/focus)C, respectively; (6) through (8) NIH(pMc*src*/coselected)A, NIH(pMc*src*/cos)B, and NIH(pMc*src*/cos)C, respectively, were metabolically labeled with [^{35}S]methionine for 8 h and lysates containing equal amounts of total cell protein of roughly equal specific activities were immunoprecipitated with *src* reactive serum in antibody excess and analyzed by SDS-polyacrylamide gel electrophoresis and autoradiography as described in the text. Densitometer tracings show that the relative intensities of the pp60^{src} bands are (lanes 1 through 6) 0:1:4:5:5.5:1.5:1:1. (M.W., molecular weight standards.)

identical to that obtained with pp60$^{c\text{-}src}$ from ^{32}P-labeled chicken embryo fibroblasts and, as expected, had smaller carboxyl fragments than did pp60$^{v\text{-}src}$. (Figure 5 shows an example of Cleveland digests from one line of each type.) This showed that there were no gross rearrangements of the overexpressed c-*src* genes even in the focus-selected cells. Twice as much radioactivity was located in the immunoprecipitated pp60^{src} bands from the NIH(pMc*src*/focus) cells relative to the NIH(pMc-*src*/cos) cells (data not shown). Since there is twice as much pp60$^{c\text{-}src}$ in the focus-selected as in the coselected overexpressor cells, we conclude that the molar ratio of phosphate to pp60$^{c\text{-}src}$ is the same in both types of overexpressor cells.

Comparison of specific in vitro kinase activities of pp60$^{c\text{-}src}$ from coselected and focus-selected overexpressor cells. The specific activity of pp60$^{c\text{-}src}$ phosphorylation for most exogenous substrates is significantly less than that of pp60$^{v\text{-}src}$ (13a; Coussens et al., submitted for publication; H. Iba and H. Hanafusa, personal communication). To investigate the possibility that c-*src* mutation in the focus-selected c-*src* overexpressor cells had resulted in the generation of a pp60^{src} with high kinase specific activity, we compared the in vitro autophosphorylation and exogenous substrate kinase activities of pp60$^{c\text{-}src}$ immunoprecipitated from coselected and focus-selected cell lysates by using monoclonal antibody MAb327 (18). Since these assays must be performed in excess antigen (J. Brugge, personal communication), the amounts of cell lysate used were adjusted (according to the measured protein equilibrium levels) so that each reaction contained equal amounts of pp60^{src} (except for the NIH 3T3 control). The results obtained with enolase as exogenous substrate are shown in Fig. 6 and demonstrate that the autophosphorylating and enolase phosphorylating activities of pp60$^{c\text{-}src}$ from both the coselected and focus-selected cells are equal. The kinase activities of pp60$^{c\text{-}src}$ and pp60$^{v\text{-}src}$ are compared in detail in a separate report (Coussens et al., submitted for publication), but it can be seen here that pp60$^{c\text{-}src}$ and pp60$^{v\text{-}src}$ have approximately equal autophosphorylating activity, even though they differ significantly in enolase and immunoglobulin G phosphorylating activity.

Focus-forming assays of secondary transfections. If the integrated c-*src* genes which induced focus formation in the NIH(pMc*src*/focus) cells did so because they had been mutated into highly transforming variants, we would expect that secondary transfection of these integrated modified genes would generate foci with frequencies comparable to

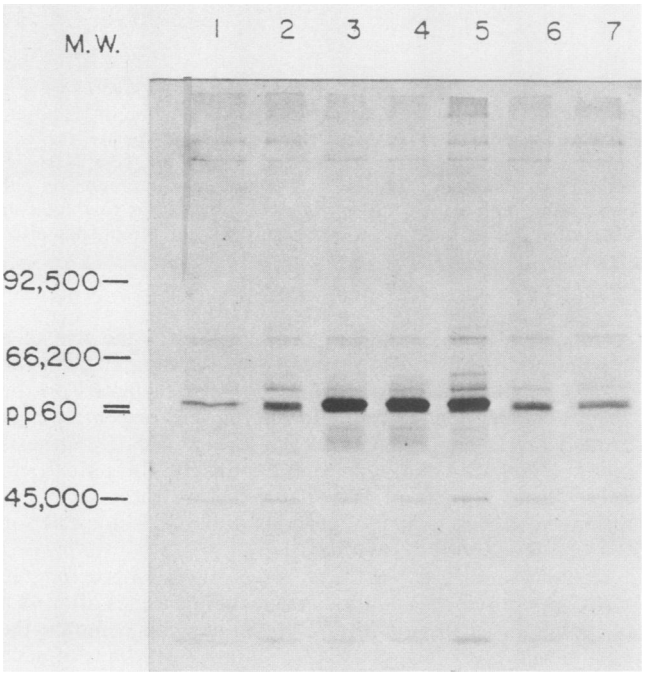

FIG. 4. Comparative pp60^{src} immunoprecipitations from focus-selected and coselected c-*src* and v-*src* overexpressor cells; long-term label. Cells from biological clones (1) NIH 3T3, (2) NIH(p*src*11), (3) NIH(pMc*src*/focus)A, (4) NIH(pMc*src*/focus)B, (5) NIH(pMc*src*/cos)A, (6) NIH(pMv*src*/focus)A, and (7) NIH(pMv*src*/cos)A were metabolically labeled with [^{35}S]methionine for 48 h. Lysates containing equal amounts of total cell protein of roughly equal specific activities were immunoprecipitated with *src* reactive serum in antibody excess and analyzed by SDS-polyacrylamide gel electrophoresis and autoradiography as described in the text. The doublets appearing in lanes 2, 6, and 7 correspond to the endogenous mouse pp60$^{c\text{-}src}$ (above) and plasmid-generated pp60$^{v\text{-}src}$ (below). Densitometer tracings show that the relative intensities of the pp60^{src} bands (after subtracting for endogenous mouse pp60$^{c\text{-}src}$ in lanes 2 through 7) are (lanes 1 through 7) 0.5:1:7:10:5:1:1. (M.W., molecular weight standards.)

those obtained by secondary transfection of integrated v-*src* genes from NIH(pMv*src*/focus) cells. Alternatively, if the integrated c-*src* genes were not modified, we would expect low secondary transfection focus-forming activities comparable to those obtained by transfecting the presumably unmodified c-*src* genes in the NIH(pMc*src*/cos) cells. (This assumes that the factors responsible for the very high level of c-*src* expression in the focus-selected cells were not closely linked to the integrated c-*src* genes.) Therefore, we performed secondary transfections with DNAs isolated from the c-*src* and v-*src* coselected and focus-selected cell lines to provide additional data about the state of the integrated c-*src* genes in the focus-selected cells. The strategy of this experiment is illustrated in Fig. 7. Both the focus-selected and coselected c-*src* cell line DNAs induced low levels of focus formation relative to both the focus-selected and coselected v-*src* cell line DNAs which induced approximately equal, high levels of focus formation (Table 1).

Comparison of the biological phenotypes of the pp60^{src} overexpressor cells. Since the NIH(pMc*src*/cos) cells had been isolated at subconfluent densities, we did not know whether they would form foci in monolayer culture. Cell mixing experiments were performed for this purpose. Cells from coselected and focus-selected c-*src* and v-*src* overexpressor biologically cloned lines were trypsinized from monolayer cultures, mixed with an excess of normal NIH 3T3 cells, plated into tissue culture dishes, and observed after 7 to 10 days for the appearance of foci in competitive monolayer culture in media supplemented with either 5 or 10% calf serum. Duplicate plates containing 50, 500, or 5,000 overexpressor cells with 5×10^5 NIH 3T3 cells were assayed for each cell line. The results are given in Table 2, and typical foci are shown in Fig. 2. In contrast with the coselected and focus-selected v-*src* expressor cells, which all formed foci, only the focus-selected but not the coselected c-*src* expressor cells formed foci. Rare colonies of modified cells could be identified in the plates containing coselected c-*src* overexpressor cells (Fig. 2), but these cells did not form true foci characterized by disorganized multilayered cell growth. Approximately 2% of the plated coselected c-*src* overexpressor test cells generated such colonies. No significant difference was observed between experiments carried out in media supplemented with either 5 or 10% serum.

In contrast with the focus-forming results, both the morphologies and the anchorage-independent growth characteristics of the coselected and focus-selected c-*src* overexpressor cells were similar and intermediate between those of normal NIH 3T3 cells and v-*src* transformed cells (Fig. 2).

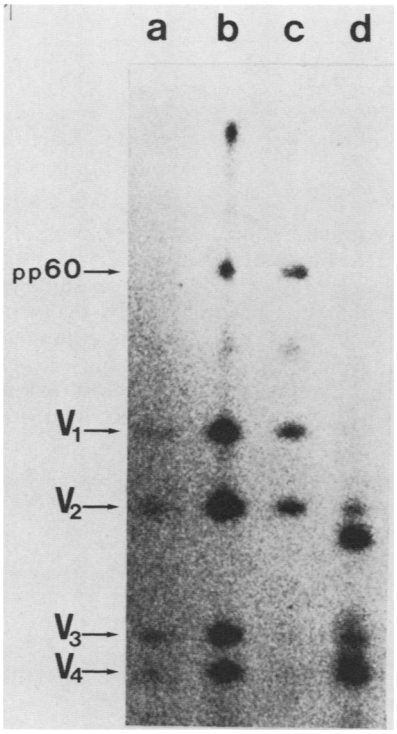

FIG. 5. Cleveland digests of overexpressed pp60$^{c\text{-}src}$. pp60$^{c\text{-}src}$ was immunoprecipitated from cells metabolically labeled with ^{32}P and subjected to Cleveland digestion, SDS-polyacrylamide gel electrophoresis, and autoradiography, as described in the text. Cell types: (a) chicken embryo fibroblast secondary culture, (b) NIH(pMc*src*/focus)B, (c) NIH(pMc*src*/cos)A, and (d) NIH(pMv*src*/focus)A. The arrows indicate the positions of uncut pp60$^{c\text{-}src}$ (pp60), the 34-kd amino terminal fragment (V1), the 26-kd carboxyl terminal fragment (V2), and two fragments, V3 and V4, resulting from further cleavage of the 34-kd amino terminal fragment. These fragments had molecular sizes of 20 and 18 kd, respectively. The uncut pp60^{src} and amino V1 bands were completely digested and do not appear in lane d. The dark V2 carboxyl fragment in lane d comes from pp60$^{v\text{-}src}$, and the light band just above it comes from the endogenous mouse pp60$^{c\text{-}src}$.

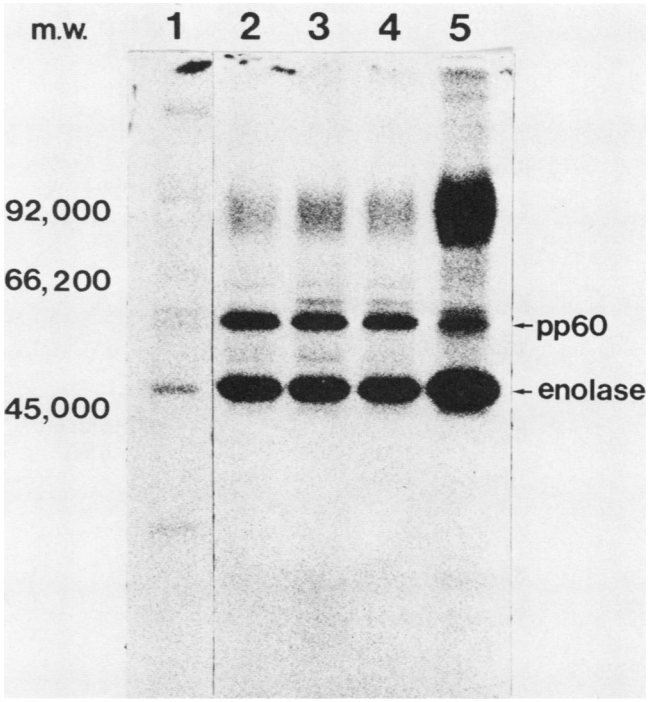

FIG. 6. Comparison of the specific kinase activities of pp60$^{c\text{-}src}$ from coselected and focus-selected overexpressor cells. Cell lysates adjusted to contain equal amounts of pp60^{src} protein were immunoprecipitated in antigen excess with anti-*src* monoclonal antibody MAb327 (18). Immunoprecipitates were assayed for in vitro autophosphorylation and enolase kinase activity by using [γ-^{32}P]ATP, as described in the text. The lysate sources and amounts of total cell protein used were: (1) NIH 3T3, 1,000 μg; (2) NIH(pMc*src*/focus)B, 143 μg; (3) NIH(pMc*src*/cos)A, 250 μg; (4) NIH(pMc*src*/cos)B, 250 μg; (5) NIH(pMv*src*/cos)A, 1,000 μg. Products of the kinase reactions were analyzed by SDS-polyacrylamide gel electrophoresis and autoradiography, as described in the text. The high-molecular-weight phosphorylated band is probably rabbit anti-mouse immunoglobulin G.

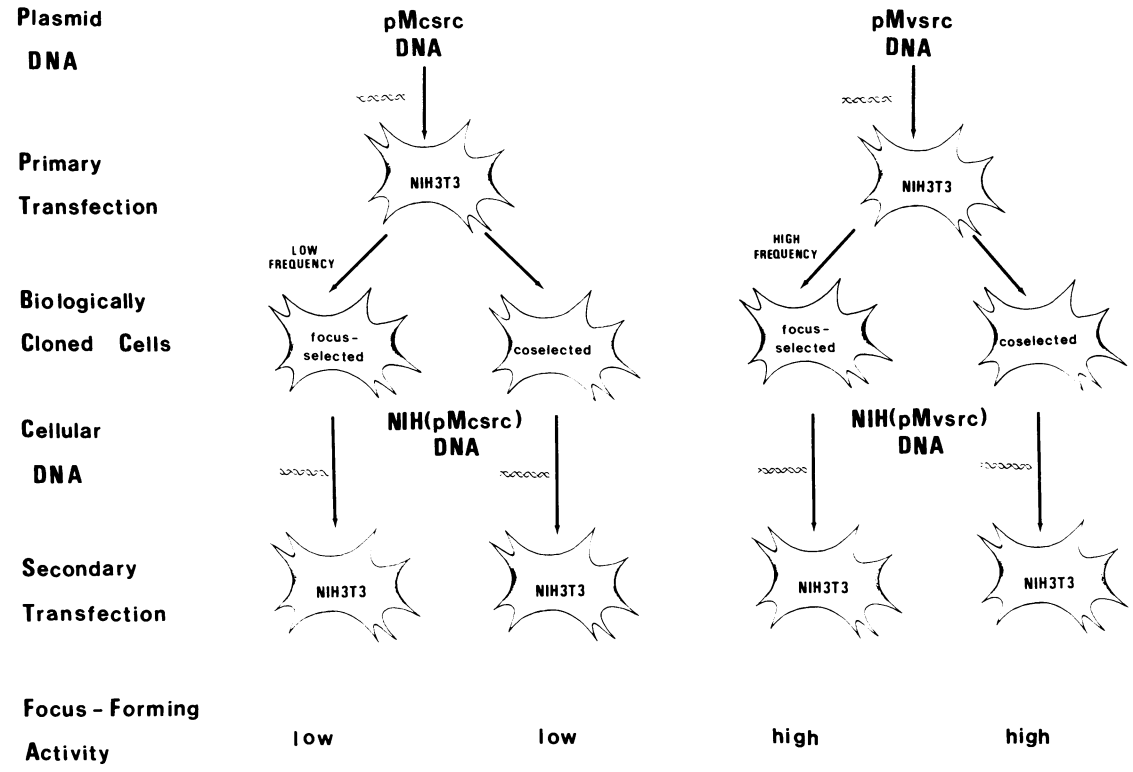

FIG. 7. Strategy of c-*src* secondary transfection experiments. Focus-forming activities are given in Table 1.

Anchorage-independent growth was assayed by plating the cell lines into media containing 0.25% agarose and either 5 or 10% calf serum. Most of the c-*src* overexpressor cell lines, both coselected and focus selected, formed small colonies, as opposed to the NIH 3T3 cells which formed no colonies at all and the v-*src* coselected and focus-selected cells which formed large colonies. Although the colonies formed by the v-*src* overexpressor cells continued to grow without limit, the colonies formed by the c-*src* overexpressor cells did not grow beyond the limits shown in Fig. 2. Colony formation by the c-*src* overexpressor cells was a somewhat variable phenomenon that was not induced by every c-*src* overexpressor line and varied in extent from experiment to experiment, even in the lines which did induce it. The examples shown in Fig. 2 represent the greatest extent of colony formation which was observed in six independent experi-

TABLE 2. Biological comparison of transfected cell lines[a]

Cell line	Transfected gene	Selection method	Focus-forming efficiency in cell-mixing expts	Colony formation in soft agrose[b]	In vivo tumorigenicity (no. of tumors/ no. injected)[c]
NIH 3T3			0	−	0/8
NIH(p*src*11)	RSV LTR/v-*src*	Focus	0.4	+++	ND[d]
NIH(pMv*src*/focus)A	MoMLV LTR/v-*src*	Focus	0.4	+++	5/6
NIH(pMv*src*/focus)B	MoMLV LTR/v-*src*	Focus	0.1	+++	ND
NIH(pMv*src*/focus)C	MoMLV LTR/v-*src*	Focus	0.2	+++	ND
NIH(pMv*src*/cos)A	MoMLV LTR/v-*src*	Coselected	0.4	+++	ND
NIH(pMc*src*/focus)A	MoMLV LTR/c-*src*	Focus	0.3	+/−	0/8
NIH(pMc*src*/focus)B	MoMLV LTR/c-*src*	Focus	0.2	+	0/8
NIH(pMc*src*/focus)C	MoMLV LTR/c-*src*	Focus	0.6	+	ND
NIH(pMc*src*/cos)A	MoMLV LTR/c-*src*	Coselected	0	+	ND
NIH(pMc*src*/cos)B	MoMLV LTR/c-*src*	Coselected	0	+/−	ND
NIH(pMc*src*/cos)C	MoMLV LTR/c-*src*	Coselected	0	−	ND

[a] Cell lines were cloned from transfected cells and analyzed as described in the text. Focus-forming efficiencies in cell mixing experiments were determined by counting the number of foci which appeared 10 days after mixing and plating 50 to 5,000 test cells with 5×10^5 NIH 3T3 cells and dividing by the number of test cells added to the plate. Averages from multiple experiments with duplicate plates were compiled by using data from plates having 0 to 100 foci.

[b] Colony formation in soft agarose is rated on a scale for which (referring to Fig. 2, row B) +++, phenotype displayed in the NIH(pMv*src*) panels (unlimited growth in soft agarose of >30% of the cells); +, phenotype displayed in the NIH(pMc*src*) panels (limited growth in soft agarose of >10% of the cells) or in the NIH(pCS12.13) panel of reference 28, Fig. 3; and −, phenotype displayed in the NIH 3T3 panel (no growth in soft agarose); +/−, variable positive and negative results in multiple experiments.

[c] All tumors appeared within 16 days, although animals were monitored for 11 weeks.

[d] ND, Not done.

ments. Other experiments with these same cell lines gave results looking like those shown for NIH(pCS12.13) cells in Fig. 3 of Shalloway et al. (28) or no growth in soft agarose at all, as indicated in Table 2. Reduction of serum concentration to 5% significantly reduced colony formation by the c-*src* overexpressor cells (one of the focus-selected lines and all of the coselected lines formed no colonies at all) but did not have a large effect on colony formation by the v-*src* overexpressor cells.

The in vivo tumorigenicities of the focus-selected cells were assayed by subcutaneously injecting 10^6 cells per NFS mouse (Table 2). Tumors appeared in five out of six mice injected with focus-selected v-*src* transformed cells within 16 days, whereas no tumors appeared in two groups of eight mice injected with two independent lines of focus-selected c-*src* overexpressor cells even after 75 days.

DISCUSSION

Transfection of NIH 3T3 mouse cells with an expression plasmid, pMc*src*, which uses MoMLV LTRs for efficient expression of chicken c-*src* resulted in focus formation at about 1% the frequency of focus formation induced by a similar v-*src* expression plasmid, pMv*src*. Coselected cell lines overexpressed pp60$^{c\text{-}src}$ but did not form foci in cell-mixing experiments, consistent with the hypothesis that they represented the phenotypically undistinguished ≥99% of the pMc*src* transfection events.

Immunoprecipitation with *src* antisera and Cleveland digestion with *S. aureus* V-8 protease of cell lysates metabolically labeled with ^{32}P showed that both the focus-selected and coselected c-*src* overexpressor cells were expressing proteins that were indistinguishable at this level of resolution from normal chicken pp60$^{c\text{-}src}$. pp60$^{c\text{-}src}$ from both the focus-selected and coselected overexpressor cells had equal specific kinase activities in vitro when bound in the immune complex. (An extensive comparison of the overexpressed pp60$^{c\text{-}src}$ and pp60$^{v\text{-}src}$ kinase activities is presented by Cousens et al. [submitted for publication].) Quantitative comparison of immunoprecipitates from cells metabolically labeled with [^{35}S]methionine showed that the synthesis rate of pp60$^{c\text{-}src}$ in the three focus-selected cell lines was about 4 times as high as the rate in the three coselected c-*src* overexpressor cell lines. This suggested that the relatively rare c-*src*-induced focus-forming events were caused by rare transfection events which resulted in very high level pp60$^{c\text{-}src}$ expression amid a background of many more transfection events which caused more moderate pp60$^{c\text{-}src}$ overexpression without focus formation.

This hypothesis was supported by secondary transfection experiments which showed that the DNAs purified from both the focus-selected c-*src* and coselected pp60$^{c\text{-}src}$ overexpressor cells had low focus-forming activities compared with DNAs from both the focus-selected and coselected pp60$^{v\text{-}src}$ transformed cells. DNAs purified from the focus-selected or coselected c-*src* overexpressor cells had about 1% focus-forming activity relative to DNAs purified from v-*src* overexpressor cells, as would be predicted from the focus-forming activities of the plasmid DNAs if no mutations had occurred.

Control experiments with pMv*src* transfected cells showed no differences between focus-selected and coselected cells when v-*src* rather than c-*src* was being overexpressed. Both types of v-*src* expressor cells had similar expression levels and biological phenotypes (focus formation, morphology, and growth in soft agarose). It is interesting that pMv*src* did not induce significantly more v-*src* expression than plasmid p*src*11 but that it had about 15-fold higher focus-forming activity. This may reflect differences in the Schmidt-Ruppin A (expressed by pMv*src*) and Schmidt-Ruppin D (produced by p*src*11) v-*src* transforming activities or may reflect the existence of a relatively sharp v-*src* expression level transformation threshold that lies between the average p*src*11- and pMv*src*-induced expression levels. Alternatively, the presence of the MoMLV LTRs may enhance the integration frequency of pMv*src* (and also pMc*src*) relative to that of p*src*11.

Comparison of the immunoprecipitations from short- and long-term metabolically labeled cells supports the recent finding that the pp60$^{c\text{-}src}$ metabolic half-life (about 20 to 24 h) (13a, 24) is significantly longer than the pp60$^{v\text{-}src}$ metabolic half-life (7 h) (27). The equilibrium levels of pp60$^{v\text{-}src}$ in the transformed cells were surprisingly low, only about 1.5 times the levels of endogenous mouse pp60$^{c\text{-}src}$, and emphasize the relative potency of pp60$^{v\text{-}src}$ as a transforming agent.

The ratio of pp60$^{c\text{-}src}$ equilibrium levels in the focus-selected and coselected c-*src* overexpressor cells is only 2:1, in contrast to the ratio of synthesis rates, which is about 4:1. This probably reflects reduced in vivo stability of the rapidly synthesized pp60$^{c\text{-}src}$ in the focus-selected cells relative to the more moderately synthesized pp60$^{c\text{-}src}$ in the coselected cells and suggests interesting hypotheses for further experimentation. For example, the effect might be due to saturation of the normal cellular complexing sites for pp60$^{c\text{-}src}$, resulting in reduced stability of the uncomplexed overexpressed molecules. This hypothesis could also account for the reduced pp60$^{v\text{-}src}$ in vivo half-life if it is not bound in the normal cellular complexing sites at any concentration. If such putative sites are also involved in pp60^{src} down regulation, differences beween pp60$^{v\text{-}src}$, pp60$^{c\text{-}src}$, and highly overexpressed pp60$^{c\text{-}src}$ complexing could account for the observed differences in in vivo protein-tyrosine phosphorylating and transforming activities.

Focus-forming activity aside, the biological phenotypes of the focus-selected and coselected c-*src* overexpressor cells appeared to be similar but distinct from that of normal NIH 3T3 cells. Both types of cells formed small colonies of restricted growth in soft agarose, had morphologies that were intermediate between those of normal and v-*src* transformed cells, and were not tumorigenic in NFS mice. The phenotype observed with the coselected MoMLV LTR promoter c-*src* overexpressor cells was similar to that previously observed with coselected simian virus 40 promoter–c-*src* overexpressor cells, which had even lower levels of protein expression (28, 29). The biological parameters of *src*-induced transformation can be separated into at least three groups of effects which progressively appear in response to increasing oncogenic stimuli. In order, these are (i) intermediate morphology and limited growth in soft agarose, (ii) focus formation, and (iii) completely transformed morphology, unlimited growth in soft agarose, and in vivo tumorigenicity.

The finding that pp60$^{c\text{-}src}$ has focus-forming activity shows that it is not totally inert as a transforming agent and suggests that pp60$^{v\text{-}src}$-induced transformation represents a perturbation of already existent pp60$^{c\text{-}src}$-related molecular control processes. This opens the possibility that even higher levels of pp60$^{c\text{-}src}$ overexpression could induce a completely transformed phenotype. Whether or not this is true, these results demonstrate that the different parameters of transformation can respond in noncoordinate fashion to quantitative and qualitative modifications in proto-oncogene

expression, that at least two separable functional activities are required even for transformation of an immortalized cell line, and that pp60$^{c\text{-}src}$ has at least one and lacks at least one of these activities when expressed at the described levels.

ACKNOWLEDGMENTS

We thank T. Kmiecik for assistance in transfections, J. Brugge for providing monoclonal and polyclonal antisera, A. D. Zelenetz and G. M. Cooper for providing clone p*src*11, and H. Hanafusa for providing clone pN4.

This work was supported by Public Health Service grant CA32317 from the National Institutes of Health, an American Cancer Society Junior Faculty Research Award to D.S., and a generous gift from E. Shapiro.

LITERATURE CITED

1. **Bishop, J. M., and H. Varmus.** 1982. Functions and origins of retroviral transforming genes, p. 999–1108. *In* R. Weiss, N. Teich, H. Varmus, and J. Coffin (ed.), RNA tumor viruses: molecular biology of tumor viruses (2nd ed.). Cold Spring Harbor Laboratory, Cold Spring Harbor, N.Y.
2. **Bishop, J. M., and H. E. Varmus.** 1984. Functions and origins of retroviral transforming genes, p. 249–346. *In* R. Weiss, N. Teich, H. Varmus, and J. Coffin (ed.), RNA tumor viruses: molecular biology of tumor viruses (suppl.). Cold Spring Harbor Laboratory, Cold Spring Harbor, N.Y.
3. **Blair, D. G., M. Oskarsson, T. G. Wood, W. L. McClements, P. J. Fischinger, and G. F. Vande Woude.** 1981. Activation of the transforming potential of a normal cell sequence: a molecular model for oncogenesis. Science **212**:941–943.
4. **Bolen, J. B., C. J. Thiele, M. A. Israel, W. Yonemoto, L. A. Lipsich, and J. S. Brugge.** 1984. Enhancement of cellular *src* gene product associated tyrosyl kinase activity following polyoma virus infection and transformation. Cell **38**:767–777.
5. **Calos, M. P., J. S. Lebkowski, and M. R. Botchan.** 1983. High mutation frequency in DNA transfected into mammalian cells. Proc. Natl. Acad. Sci. U.S.A. **80**:3015–3019.
6. **Cleveland, D. W., S. G. Fischer, M. W. Kirschner, and U. K. Laemmli.** 1977. Peptide mapping by limited proteolysis in sodium dodecyl sulfate and analysis by gel electrophoresis. J. Biol. Chem. **252**:1102–1106.

6a. **Cooper, J. A., T. Hunter, and D. Shalloway.** 1985. Protein-tyrosine kinase activity of pp60$^{c\text{-}src}$ is restricted in intact cells, p. 321–328. *In* J. Feramisco, B. Ozanne, and C. Stiles (ed.), Cancer cells, vol. 3. Cold Spring Harbor Laboratory, Cold Spring Harbor, N.Y.

7. **Courtneidge, S. A., and A. E. Smith.** 1983. Polyoma virus transforming protein associates with the product of the c-*src* cellular gene. Nature (London) **303**:435–439.
8. **Czernilofsky, A. P., A. D. Levinson, H. E. Varmus, J. M. Bishop, E. Tisher, and H. M. Goodman.** 1983. Corrections to the nucleotide sequence of the *src* gene of Rous sarcoma virus. Nature (London) **301**:736–738.
9. **DeFeo, D., M. A. Gonda, H. A. Young, E. H. Chang, D. R. Lowy, E. M. Scolnick, and R. W. Ellis.** 1981. Analysis of two divergent rat genomic clones homologous to the transforming gene of Harvey murine sarcoma virus. Proc. Natl. Acad. Sci. U.S.A. **78**:3328–3332.
10. **Gilmer, T. M., and R. L. Erikson.** 1983. Development of anti-pp60^{src} serum with antigen produced in *Escherichia coli*. J. Virol. **45**:462–465.
11. **Hanafusa, H.** 1977. Cell transformation by RNA tumor viruses, p. 401–483. *In* H. Fraenkel-Conrat and R. R. Wagner (ed.), Comprehensive virology. Plenum Publishing Corp., New York.
12. **Hanafusa, H., H. Iba, T. Takeya, and F. R. Cross.** 1984. Transforming activity of the c-*src* gene, p. 1–8. *In* G. F. Vande Woude, A. J. Levine, W. C. Topp, and J. D. Watson, (ed.), Cancer cells, vol. 2. Cold Spring Harbor Laboratory, Cold Spring Harbor, New York.
13. **Heldin, C.-H., and B. Westermark.** 1984. Growth factors: mechanism of action and relation to oncogenes (review). Cell **37**:9–20.

13a. **Iba, H., F. Cross, E. Garber, and H. Hanafusa.** 1985. Low level of cellular protein phosphorylation by overproduced p60$^{c\text{-}src}$. Mol. Cell. Biol. **5**:1058–1066.

14. **Iba, H., T. Takeya, F. R. Cross, T. Hanafusa, and H. Hanafusa.** 1984. Rous sarcoma virus variants that carry the cellular *src* gene instead of the viral *src* gene cannot transform chicken embryo fibroblasts. Proc. Natl. Acad. Sci. U.S.A. **81**:4424–4428.
15. **Kriegler, M., C. F. Perez, C. Hardy, and M. Botchan.** 1984. Transformation mediated by the SV40 T antigens: separation of the overlapping SV40 early genes with a retroviral vector. Cell **38**:483–491.
16. **Laemmli, U. K.** 1970. Cleavage of structural proteins during the assembly of the head of bacteriophage T4. Nature (London) **227**:680–685.
17. **Lebkowski, J. S., R. B. DuBridge, E. A. Antell, K. S. Greisen, and M. P. Calos.** 1984. Transfected DNA is mutated in monkey, mouse, and human cells. Mol. Cell Biol. **4**:1951–1960.
18. **Lipsich, L. A., A. J. Lewis, and J. S. Brugge.** 1983. Isolation of monoclonal antibodies that recognize the transforming proteins of avian sarcoma viruses. J. Virol. **48**:352–360.
19. **Maniatis, T., E. F. Fritsch, and J. Sambrook.** 1982. Molecular cloning: a laboratory manual. Cold Spring Harbor Laboratory, Cold Spring Harbor, N.Y.
20. **Miller, A. D., T. Curran, and I. M. Verma.** 1984. c-*fos* protein can induce cellular transformation: a novel mechanism of activation of a cellular oncogene. Cell **36**:51–60.
21. **Mulligan, R. C., and P. Berg.** 1980. Expression of a bacterial gene in mammalian cells. Science **209**:1422–1427.
22. **Oskarsson, M., W. L. McClements, D. G. Blair, J. V. Maizel, and G. F. Vande Woude.** 1980. Properties of a normal mouse cell DNA sequence of Moloney sarcoma virus. Science **207**: 1222–1224.
23. **Parker, R. C., R. Swanstrom, H. E. Varmus, and J. M. Bishop.** 1984. Transduction and alteration of a cellular gene (c-*src*) created an RNA tumor virus: the genesis of Rous sarcoma virus, p. 19–26. *In* G. F. Vande Woude, A. J. Levine, W. C. Topp and J. D. Watson (ed.), Cancer cells, vol. 2. Cold Spring Harbor Laboratory, Cold Spring Harbor, N.Y.
24. **Parker, R. C., H. E. Varmus, and J. M. Bishop.** 1984. Expression of v-*src* and chicken c-*src* in rat cells demonstrates qualitative differences between pp60$^{v\text{-}src}$ and pp60$^{c\text{-}src}$. Cell **37**:131–139.
25. **Schwartz, D., R. Tizard, and W. Gilbert.** 1983. Nucleotide sequence of Rous sarcoma virus. Cell **32**:853–869.
26. **Sefton, B. M., T. Hunter, K. Beemon, and W. Eckhart.** 1980. Phosphorylation of tyrosine is essential for cellular transformation by Rous sarcoma virus. Cell **20**:807–816.
27. **Sefton, B. M., T. Patschinsky, C. Berdot, T. Hunter, and T. Elliott.** 1982. Phosphorylation and metabolism of the transforming protein of Rous sarcoma virus. J. Virol. **41**:813–820.
28. **Shalloway, D., P. M. Coussens, and P. Yaciuk.** 1984. Overexpression of the c-*src* protein does not induce transformation of NIH3T3 cells. Proc. Natl. Acad. Sci. U.S.A. **81**:7071–7075.
29. **Shalloway, D., P. M. Coussens, and P. Yaciuk.** 1984. c-*src* and *src* homolog overexpression in mouse cells, p. 9–17. *In* G. F. Vande Woude, A. J. Levine, W. C. Topp, and J. D. Watson (ed.), Cancer cells, vol. 2. Cold Spring Harbor Laboratory, Cold Spring Harbor, N.Y.
30. **Shalloway, D., A. D. Zelenetz, and G. M. Cooper.** 1981. Molecular cloning and characterization of the chicken gene homologous to the transforming gene of Rous sarcoma virus. Cell **24**:531–541.
31. **Swanstrom, R., R. C. Parker, H. E. Varmus, and J. M. Bishop.** 1983. Transduction of a cellular oncogene: the genesis of Rous sarcoma virus. Proc. Natl. Acad. Sci. U.S.A. **80**:2519–2523.
32. **Takeya, T., R. A. Feldman, and H. Hanafusa.** 1982. DNA sequence of the viral and cellular *src* gene of chickens. I. Complete nucleotide sequence of an *Eco*RI fragment of recovered avian sarcoma virus which codes for gp37 and pp60^{src}. J. Virol. **44**:1–11.
33. **Takeya, T., and H. Hanafusa.** 1983. Structure and sequence of the cellular gene homologous to the RSV *src* gene and the mechanism for generating the transforming virus. Cell

32:881–890.
34. **Wake, C. T., T. Gudewicz, T. Porter, A. White, and J. H. Wilson.** 1984. How damaged is the biologically active subpopulation of transfected DNA? Mol. Cell. Biol. **4**:387–398.
35. **Wilhelmsen, K. C., W. G. Tarpley, and H. M. Temin.** 1984. Identification of some of the parameters governing transformation by oncogenes in retroviruses, p. 303–308. *In* G. F. Vande Woude, A. J. Levine, W. C. Topp, and J. D. Watson (ed.), Cancer cells, vol. 2. Cold Spring Harbor Laboratory, Cold Spring Harbor, N.Y.